Formation of CeSiO 4 from cerium(iii) silicate precursors

Paul Estevenon, Thibault Kaczmarek, Fabien Vadot, Thomas Dumas, Pier Lorenzo Solari, Éléonore Welcomme, Stephanie Szenknect, Adel Mesbah, Philippe Moisy, Christophe Poinssot, et al.

Formation of $CeSiO_4$ from cerium(III) silicate precursors

Paul Estevenon[a,b], Thibault Kaczmarek[a,b], Fabien Vadot[a,b], Thomas Dumas[a], Pier Lorenzo Solari[c], Eleonore Welcomme[a], Stephanie Szenknect[b], Adel Mesbah*[b], Philippe Moisy[a], Christophe Poinssot[a], Nicolas Dacheux*[b]

Even if the preparation of $CeSiO_4$ has already been reported, the formation of pure cerium silicate from aqueous precursors appears as a challenge. An innovative way of synthesis has been identified in this study allowing the formation of $CeSiO_4$ after hydrothermal treatment starting from Ce(III) silicate precursors. Among the experimental parameters examined, significant effects were found according to the nature of the precursor and reactive media considered, pH of the reactive media and temperature of the hydrothermal process. This study allows to determine optimized conditions for the hydrothermal synthesis of pure $CeSiO_4$ (A-$Ce_2Si_2O_7$ or $Ce_{4.67}(SiO_4)_3O$ as starting precursors, nitric medium, pH = 7, 7 days at 150°C). In situ low oxidation rate of Ce(III) into Ce(IV) was a key parameter to consider in order to avoid the presence of CeO_2 in the final mixtures.

Introduction

Cerium is often considered as a convenient surrogate in order to determine the behavior of plutonium in various systems, because Ce(III) and Ce(IV) chemistry are close to their plutonium counterparts and relatively representative of Pu(IV)/Pu(III) redox couple (E°(Ce(IV)/Ce(III) = 1.72 V/ENH;[1] E°(Pu(IV)/Pu(III) = 1.047 ± 0,003 V/ENH [2]). In particular, Ce(III) silicate phases may be used to simulate isostructural Pu(III) silicates, which have been reported in few studies only.[3-5] $CeSiO_4$ is also isostructural of $ZrSiO_4$, $HfSiO_4$ and $AnSiO_4$ (for An = Th, Pa, U, Np, Pu and Am) [6-9] (space group $I4_1/amd$). The formation of actinide silicate colloids was observed at room temperature for thorium, uranium(IV) and neptunium(IV) and was proved to modify the mobility of the actinides in the environment.[10-14] The potential formation of Pu-based colloids in conditions representative of spent nuclear fuels repository settings deserves to be investigated. In this context, the study of cerium silicates appears as a compulsory first step to evaluate the behavior of plutonium in silicate-rich environments submitted to various redox conditions.

The preparation and characterization of Ce(III) silicates (Ce_2SiO_5, $Ce_{4.67}(SiO_4)_3O$, A-$Ce_2Si_2O_7$ and G-$Ce_2Si_2O_7$) by high temperature routes has been extensively studied due to their potential applications.[15-25] Indeed, these compounds have been identified as promising luminescent materials (in the blue/violet region) for scintillators and detectors applications.[21-25] They have also been identified as very efficient ions exchangers for radionuclides separation [20] and their formation has been reported as secondary phases for cerium doped zircon ceramics and cerium doped nuclear waste glasses.[26, 27] However, the behavior of Ce(III) silicate phases in wet reactive media has not been studied so far.

$CeSiO_4$ has been reported by Schlüter et al.[28] as a natural occurring mineral phase formed in pegmatite rocks of the Stetind mount (Norway). The first synthesis of this silicate was reported by Dickson and Glasser in 2000 [9, 29]. It consisted in the hydrothermal treatment of a mixture containing $Ce(NO_3)_3$, SiO_2 and CaO under inert atmosphere between 55 and 180°C. The formation of $CeSiO_4$ samples using a wet chemistry route from Ce(III) nitrate or chloride at temperatures ranging from 40°C to 150°C in weakly basic conditions has been reported recently[30]. These results highlighted that the use of Ce(III) was required to prepare $CeSiO_4$. Indeed, all the attempts to form $CeSiO_4$ from Ce(IV) precursors failed due to the precipitation of cerium tetrahydroxide, leading to CeO_2 by ageing. Consequently, the use of reactive conditions that may disfavor cerium hydrolysis constitutes a key parameter to prepare pure $CeSiO_4$. The formation of $CeSiO_4$ from crystalline Ce(III) silicate phases through a dissolution and oxidation process could also be considered as an alternative way of synthesis. Moreover, due to cerium representativity as a plutonium surrogate, this study may provide crucial information on plutonium silicate chemistry and, therefore, on the behavior of plutonium in the environment. In this context, this paper reports a comprehensive study of the formation of $CeSiO_4$ by chemical degradation of solid Ce(III) silicate precursors.

Table 1. Conditions of formation of Ce(III) silicate precursors and associated lattice parameters determined by Rietveld refinement.

Compound	Space group	Grinding step	Thermal treatment	Unit cell parameters			
				a (Å)	b (Å)	c (Å)	β (°)
Ce_2SiO_5	$P12_1/c1$ (14)	1h – 30 Hz	9h –1350°C Ar - 4% H_2	9.2775(3)	7.3942(3)	6.9665(3)	108.33(1)
$Ce_{4.67}(SiO_4)_3O$	$P6_3/m$ (176)			9.6505(4)		7.0738(3)	
A-$Ce_2Si_2O_7$	$P4_1$ (76)			6.7965(3)		24.7258(14)	
G-$Ce_2Si_2O_7$	$P2_1/n$ (14)	1h – 30 Hz	9h –1550°C Ar - 4% H_2	8.7245(4)	13.0735(6)	5.4031(3)	90.13(1)

Materials and methods

Syntheses

Reactants. All of the reagents used were of analytical grade and supplied by Sigma-Aldrich. Na_2SiO_3 was used as the silicate precursor. CeO_2 (99.9 %) and SiO_2 (99.5 %) were used as solid precursors to prepare high-temperature Ce(III) silicate phases. 0.75 mol·L^{-1} HNO_3 and HCl solutions were prepared by dilution of Sigma Aldrich ACS grade concentrated HNO_3 (70%) and HCl (37%) solutions. 8 mol·L^{-1} NaOH solution was also freshly prepared from Sigma Aldrich ACS grade NaOH (98 %) before the experiments.

Preparation of Ce(III) silicates precursors. Ce(III) silicate precursors were prepared considering the protocol described by Zec et al.[23, 24] for Ce_2SiO_5 (space group $P12_1/c1$), $Ce_{4.67}(SiO_4)_3O$ (space group $P6_3/m$), tetragonal $Ce_2Si_2O_7$ (space group $P4_1$, named "A-$Ce_2Si_2O_7$") and monoclinic $Ce_2Si_2O_7$ (space group $P2_1/n$, named "G-$Ce_2Si_2O_7$").

The samples were prepared by mixing CeO_2 and SiO_2 in stoichiometric conditions with respect to the targeted materials. Homogenization of the powders was performed by mechanical milling step (30 Hz, 1 hour) in a tungsten carbide milling vessel thanks to a Retsch MM 200 vibration mill mixer. The samples were then pelletized by isostatic pressing under 5 MPa at room-temperature and heated at high temperature under Ar – 4% H_2 atmosphere in order to favor the cerium reduction, as described in **Table 1**.

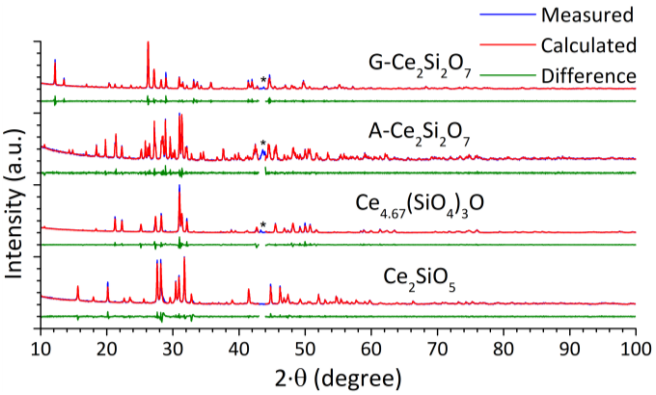

Figure 1. PXRD diagrams of prepared Ce_2SiO_5, $Ce_{4.67}(SiO_4)_3O$, A-$Ce_2Si_2O_7$ and G-$Ce_2Si_2O_7$, calculated and difference profiles after Rietveld refinement. XRD lines of sample holder are pointed out by an asterisk.

The as-prepared samples were characterized by Powder X-Ray Diffraction (PXRD), infrared and Raman spectroscopies and Scanning Electron Microscopy (SEM). The presence of cerium oxides was never detected in the samples. Moreover, Rietveld refinement of the diagrams did not show significant differences of the lattice parameters compared to those reported in the literature [19] (**Table 1**, **Table S2** and **Figure 1**). Infrared and Raman spectra were also recorded for each compound before and after hydrothermal treatment (**Figure S1** and **Figure S2**).

Preparation of $CeSiO_4$ from Ce(III) silicate precursors. Ce(III) silicate based precursors were placed in contact with 0.75 mol.L^{-1} HNO_3 or HCl solution in air (no dissolution was evidenced in these conditions). The pH was then adjusted to the final value with 8 mol·L^{-1} NaOH solution. The mixtures were put in Teflon lined reactors in Parr autoclaves and then treated in hydrothermal conditions for 1 to 20 days between 60°C to 250°C and under autogenous pressure (reference conditions were fixed to 7 days and 150°C, respectively) (**Table S1**). The obtained precipitates were then separated from the supernatant by centrifugation for 12 min at 14 000 rpm, washed twice with deionized water and once with ethanol, and finally dried overnight at 60°C in an oven. The samples were characterized by PXRD, infrared and Raman spectroscopies, SEM and XAS.

Characterization

The synthesized compounds were analyzed by PXRD with the help of a Bruker D8 advance diffractometer equipped with a lynxeye detector and using Cu Kα radiation (λ = 1.54184 Å) in a reflection geometry (parallel beam). PXRD patterns were recorded between 5° and 100° (2θ) with steps of 0.019° and a total counting time of 2.5 to 3 hours per sample. Pure silicon was used as a standard material to extract the instrumental parameters. All the collected data were refined by the Rietveld method using the Fullprof_Suite package.[31] During the refinements, different profile and structure parameters were allowed to vary, such as the zero shift, unit-cell parameters, scale factor, and overall displacement factor. However, the occupancy of each site was fixed to the calculated values.

Raman spectra were recorded with a Horiba-Jobin Yvon Aramis device equipped with an edge filter and a Nd:YAG laser (532 nm) that delivered 60 mW at the surface of the sample. In order to

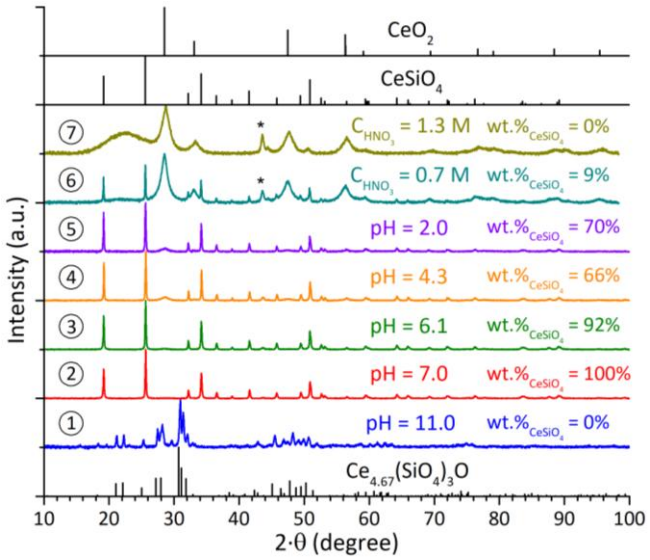

Figure 2. PXRD patterns obtained after hydrothermal treatment (7 days, T = 150°C) under air atmosphere starting from $Ce_{4.67}(SiO_4)_3O$ precursor in nitric acid media and with an initial pH equal to 11.0 (1), 7.0 (2), 6.1 (3), 4.3 (4), 2.0 (5), C_{HNO_3} = 0.7 mol·L^{-1} (6) and C_{HNO_3} = 1.3 mol·L^{-1} (7). XRD lines of the sample holder are pointed out by an asterisk. Characteristic XRD lines of CeO_2, $CeSiO_4$ and $Ce_{4.67}(SiO_4)_3O$ were extracted from ref **32**, **9** and **16**, respectively.

avoid any laser-induced degradation of the compound, the power was turned down by the means of optical filters. The laser beam was then focused on the sample using an Olympus BX 41 microscope with a X50LMP objective, resulting in a spot area of ~1 µm^2 and a power of 475 µW for $CeSiO_4$ samples and of 3.8 mW for Ce(III) silicates. For each spectrum, a dwell time ranging from 30 to 600 s was used. All the recorded spectra corresponded to the average of four scans in order to minimize the measurement error. Moreover, the data were collected on different areas for each sample.

FTIR spectra were recorded in the 300–4000 cm^{-1} range with a Perkin-Elmer FTIR Spectrum 100 device. Powdered samples were deposited on the surface of an ATR crystal without any prior preparation. The spectra collected in such operating conditions exhibited a resolution lower than 4 cm^{-1}. Four scans were performed to average the measurement error.

SEM observations were directly conducted on small powder samples without any prior preparation such as metallization, using a FEI Quanta 200 electronic microscope, equipped either with an Everhart-Thornley Detector (ETD) or a Back-Scattered Electron Detector (BSED), under high vacuum conditions with a very low accelerating voltage (2 – 3.1 kV). These conditions were chosen in order to create a beam deceleration effect that led to high resolution images.

The extended X-ray absorption fine structure (EXAFS) and X-Ray Absorption Near Edge Structure (XANES) spectroscopy measurements were carried out at the MARS Beamline at the SOLEIL synchrotron facility (Saint Aubin). The spectra were collected in the fluorescence mode at room temperature. Measurements were performed at the cerium L_{III} edge (5723 eV). Data reduction and extraction of EXAFS oscillation was performed using the Athena and Artemis package.[33] The threshold energy, E_0, was defined as the maximum of the first derivate of the absorption coefficient. Experimental EXAFS spectra were Fourier transformed using a Hanning window over the k-space range 2–10 Å^{-1}. The shell fits were performed in R-space using k^1-, k^2-, and k^3-weighting. Theoretical phase shifts and backscattering amplitudes were obtained with the ab initio code FEFF8.2 [34] using the $CeSiO_4$ structures.[9]

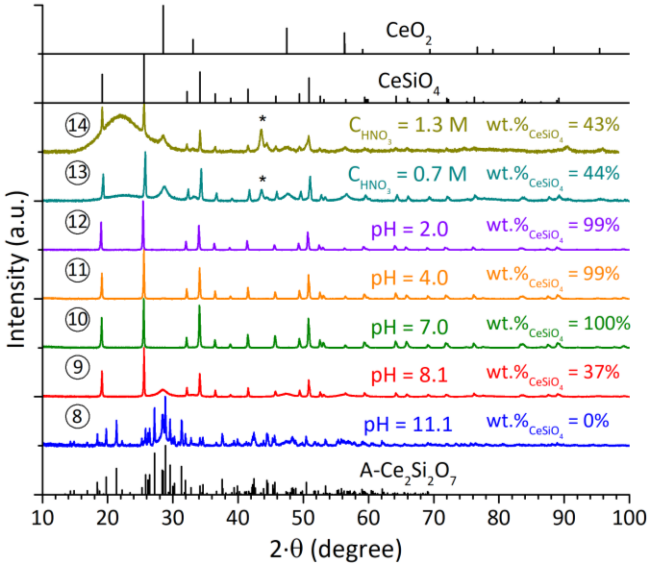

Figure 3. PXRD patterns obtained after hydrothermal treatment (7 days, T = 150°C) under air atmosphere starting from A-$Ce_2Si_2O_7$ precursor in nitric acid media and with an initial pH equal to 11.1 (8), 8.1 (9), 7.0 (10), 4.0 (11), 2.0 (12), C_{HNO_3} = 0.7 mol·L^{-1} (13) and C_{HNO_3} = 1.3 mol·L^{-1} (14). XRD lines of sample holder are pointed out by an asterisk. Characteristic XRD lines of CeO_2, $CeSiO_4$ and A-$Ce_2Si_2O_7$ were extracted from ref **32**, **9** and **24**, respectively.

Results and discussion

Preparation of $CeSiO_4$ in nitric media

All attempts to prepare $CeSiO_4$ were made from Ce_2SiO_5, $Ce_{4.67}(SiO_4)_3O$, A-$Ce_2Si_2O_7$ and G-$Ce_2Si_2O_7$ precursors and Na_2SiO_3 as complementary silicon source in order to maintain the Ce:Si stoichiometry of $CeSiO_4$.

These experiments were performed in nitric acid with 8.4 ×10^{-4} mol of cerium and silicon in 4 mL (leading to a concentration of 0.21 mol·L^{-1} when considering the full dissolution of cerium and silicon), initial acid conditions ranging from C_{HNO_3} = 1.3 mol·L^{-1} to pH = 11.7, air atmosphere and with a hydrothermal treatment of 7 days at 150°C.

For each precursor, hydrothermal treatments allowed the formation of $CeSiO_4$ on a wide pH range:

- from C_{HNO_3} = 0.7 mol·L^{-1} to pH = 8.4 starting from $Ce_{4.67}(SiO_4)_3O$ (**Figure 2**);
- from C_{HNO_3} = 1.3 mol·L^{-1} to pH = 8.1 starting from A-$Ce_2Si_2O_7$ (**Figure 3**);
- from pH = 1.0 to pH = 8.5 starting from Ce_2SiO_5 (**Figure S3**);
- from pH = 1.0 to pH = 8.2 starting from G-$Ce_2Si_2O_7$ (**Figure S4**).

The syntheses performed in very acidic media (i.e. for C_{HNO_3} > 0.3 mol·L^{-1}) usually led to the simultaneous precipitation of

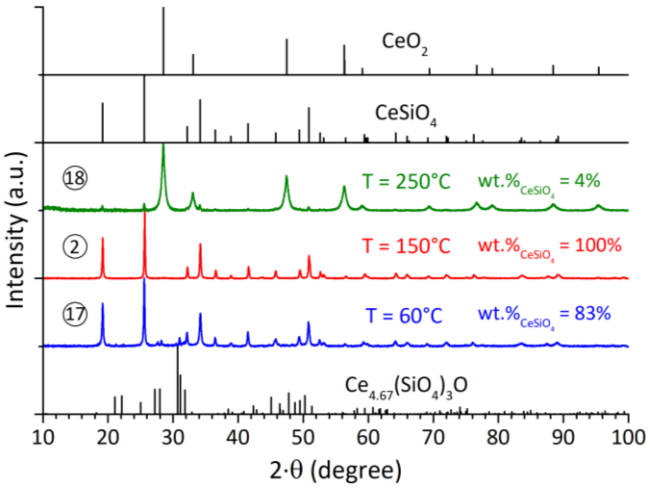

Figure 4. PXRD patterns obtained when using A-$Ce_2Si_2O_7$ as starting precursor, after hydrothermal treatment performed at 150°C under air atmosphere in nitric media and pH = 7 for 1 day (15), 3 days (16) and 7 days (10). XRD lines of sample holder are pointed out by an asterisk. Characteristic XRD lines of CeO_2, $CeSiO_4$ and A-$Ce_2Si_2O_7$ were extracted from ref **32**, **9** and **24**, respectively.

amorphous SiO_2 and solubilization of cerium as Ce^{3+} in solution. Only small amounts of cerium were precipitated as CeO_2 or $CeSiO_4$ in these conditions (mass yield below 20% compared to quasi-quantitative precipitation at higher pH).

Furthermore, hydrothermal treatments performed in alkaline media (i.e. for pH ≥ 11) did not lead to the formation of $CeSiO_4$ due to the low dissolution rate of the Ce(III) silicate based precursors. This could be directly correlated to the low solubility of these precursors in alkaline conditions due to kinetics and/or thermodynamic factors. From this point of view, performing hydrothermal treatment with an initial pH close to pH = 7 appeared as the best compromise to prepare $CeSiO_4$.

An important decrease of the pH value during the hydrothermal treatment (from initial pH = 7 to final pH = 2) was observed in conditions that favored the formation of $CeSiO_4$ (**Table S1**). However, it remains unclear whether this pH evolution was linked to the oxidation of Ce(III) species or controlled by $CeSiO_4$ solubility equilibrium.

Among the precursors used for these experiments, $Ce_{4.67}(SiO_4)_3O$ and A-$Ce_2Si_2O_7$ were the best reactants to form pure $CeSiO_4$. Indeed, using Ce_2SiO_5 as starting reactant generally led to mixtures of CeO_2 and $CeSiO_4$ (Figure S3). This result was explained by the high sensibility of Ce_2SiO_5 to oxidation compared to the other Ce(III) silicates, which could induce a fast increase of Ce(IV) concentration in solution and then, the precipitation of Ce(IV) hydroxide.[19] Using G-$Ce_2Si_2O_7$ as starting reactant in the same conditions led to mixtures of G-$Ce_2Si_2O_7$ and $CeSiO_4$. This latter result could be explained by the refractory character of G-$Ce_2Si_2O_7$ associated to lower dissolution kinetics compared to others precursors. Furthermore, kinetic studies performed on $Ce_{4.67}(SiO_4)_3O$ (Figure S5) and A-$Ce_2Si_2O_7$ (Figure 4) as starting precursors allowed to observe their complete conversion into $CeSiO_4$ after 3 days of hydrothermal treatment at 150°C in nitric media with an initial pH equal to 7.

In order to understand if the lower reactivity of G-$Ce_2Si_2O_7$ could be correlated to the temperature of the thermal treatment required to form this phase (9 hours, 1550°C, Ar – 4% H_2), syntheses of $Ce_{4.67}(SiO_4)_3O$ were also performed in the same conditions. This heating treatment did not induce any significant change in the behavior of the Ce(III) silicate precursor compared to the heating treatment performed at 1350°C. Thus, the low reactivity of G-$Ce_2Si_2O_7$ could be linked to the nature of the phase rather than to its better crystallinity or lower reactive surface area compared to others precursors.

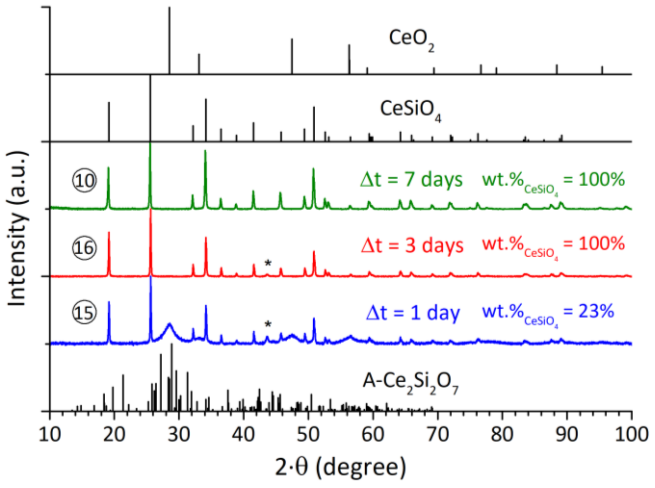

Figure 5. PXRD patterns obtained when using $Ce_{4.67}(SiO_4)_3O$ as starting precursor, after hydrothermal treatment performed under air atmosphere in nitric media and pH = 7 at 60°C (52 days) (17), 150°C (7 days) (2) and 250°C (7 days) (18). Characteristic XRD lines of CeO_2, $CeSiO_4$ and $Ce_{4.67}(SiO_4)_3O$ were extracted from ref **32, 9** and **16**, respectively.

Experiments have been also performed in order to determine if the mechanical grinding step (performed before the Ce(III) solid silicate synthesis) alone was sufficient to explain the formation of $CeSiO_4$. To this aim, hydrothermal syntheses were made at 150°C from stoichiometric amounts of CeO_2 and SiO_2 mechanically milled together for 1 hour at 30 Hz and with different pH values. $CeSiO_4$ did not form during these experiments. Therefore, the use of Ce(III) silicate precursor seems to be necessary to prepare $CeSiO_4$. This result is in good agreement with the ab initio calculation which predicts that $CeSiO_4$ is less stable than the mixture of CeO_2 and SiO_2.[35]

Because experiments performed in air led to the formation of pure $CeSiO_4$, it appeared that the working atmosphere was not a key parameter controlling the formation of $CeSiO_4$, contrarily to what was observed with the aqueous Ce(III) species.[29, 30]

The impact of the temperature of the hydrothermal treatment on the yield of formation of $CeSiO_4$ was also studied through various experiments between 60°C and 250°C starting from $Ce_{4.67}(SiO_4)_3O$ and A-$Ce_2Si_2O_7$ precursors (**Figure 5** and **Figure S6**). $CeSiO_4$ was formed between 60°C and 150°C from both precursors. At T = 250°C, a large amount of crystallized CeO_2 was formed while only small amounts of $CeSiO_4$ were obtained. Such a temperature limit is in good agreement with the one obtained from aqueous Ce(III) precursors.[30]

Moreover, thanks to SEM observations, a change in the morphology of the grains was observed during the hydrothermal treatment. Indeed, A-$Ce_2Si_2O_7$ adopted a

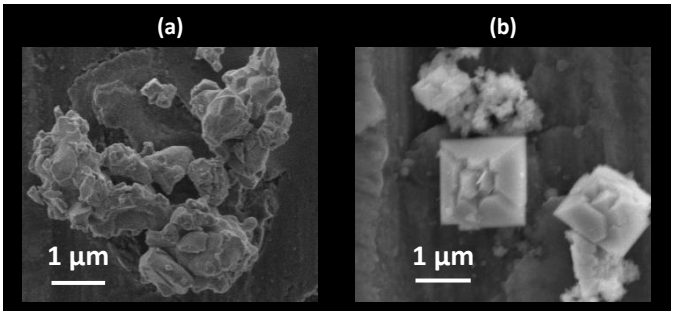

Figure 6. SEM micrograph obtained for A-$Ce_2Si_2O_7$ (T = 1350°C for 9 hours, Ar – 4% H_2) (a) and for $CeSiO_4$ obtained after hydrothermal conditions (T = 150°C, t = 7 days) under air atmosphere from A-$Ce_2Si_2O_7$, in nitric medium and pH = 7.0 (10) (b).

microstructure characteristic of sintered samples, whereas the final $CeSiO_4$ grains exhibited the square-based bipyramid morphology characteristic of zircon-type materials (**Figure 6**). The same changes were also observed during the conversion of $Ce_{4.67}(SiO_4)_3O$. Therefore, the formation of $CeSiO_4$ from Ce(III) silicate precursors surely required the progressive dissolution of the starting precursor, the oxidation of Ce(III) to Ce(IV) in solution and then, the precipitation of $CeSiO_4$.

Preparation of $CeSiO_4$ in hydrochloric media

In order to underline the potential role of nitric acid during the synthesis of $CeSiO_4$, especially through the development of redox reactions with cerium, several experiments were made from $Ce_{4.67}(SiO_4)_3O$, A-$Ce_2Si_2O_7$ and G-$Ce_2Si_2O_7$ in hydrochloric media. It should be noted that both hydrochloric and nitric acids are strong acids in this concentration range and that the complexing power of nitrate and chloride anions may be inferred to be similar.[36] In contrast, nitric acid is often an oxidizing agent while hydrochloric acid is usually considered as a more reducing medium. Hydrothermal treatments were carried out in air for 7 days at 150°C, with pH values ranging from pH = 2 to 7. All of these experiments led to the partial conversion of the starting precursors into $CeSiO_4$ (**Figure 7-a** and **Figure S7**).

As observed for G-$Ce_2Si_2O_7$, extending the duration of the hydrothermal treatment induced the increase of the yield of formation of $CeSiO_4$ (**Figure 7-b**). Therefore, it was concluded that the kinetics of formation of $CeSiO_4$ were lower in hydrochloric media than in nitric media (**Figure 2** and **Figure S7**). This difference could be attributed to the presence of nitrous acid, issued from the reduction of HNO_3, during the oxidation of Ce(III), which speeds up the kinetics of formation of $CeSiO_4$.

SEM observations performed on G-$Ce_2Si_2O_7$ and $CeSiO_4$ confirmed the morphological change already noted in nitric medium. Indeed, from the features characteristic of a sintered sample obtained for G-$Ce_2Si_2O_7$, the morphology turned into a square-based bipyramid morphology for $CeSiO_4$ (**Figure 8**). Moreover, in these conditions, which allowed a slow oxidation process, an epitaxial growth of $CeSiO_4$ was observed leading to a prism-like morphology characteristic of the zircon-type silicates growth (the spherical particles observed in **Figure 8-b** may correspond to residual G-$Ce_2Si_2O_7$ or to SiO_2).[37]

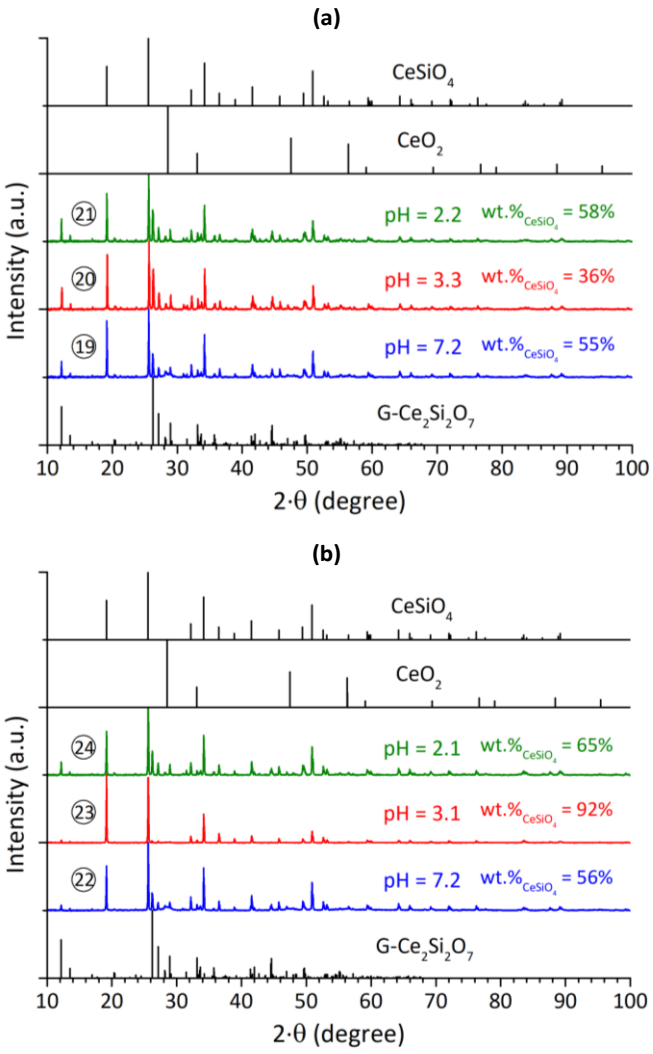

Figure 7. PXRD patterns obtained after hydrothermal treatment (7 days and T = 150°C (a) or 21 days and T = 150°C (b)) under air atmosphere starting from G-$Ce_2Si_2O_7$ precursor, in hydrochloric media and with initial pH equal to 7.2 (19), 3.3 (20), 2.2 (21), 7.2 (22), 3.1 (23) or 2.1 (24). Characteristic XRD lines of CeO_2, $CeSiO_4$ and G-$Ce_2Si_2O_7$ were extracted from ref **32, 9** and **18**, respectively.

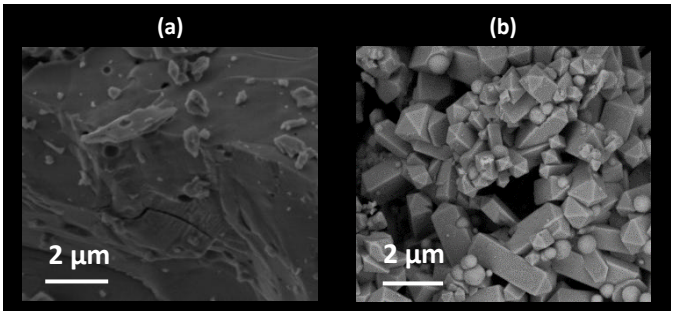

Figure 8. SEM micrograph obtained for starting G-$Ce_2Si_2O_7$ precursor (9 hours, T = 1550°C, under Ar – 4% H_2) (a) and for $CeSiO_4$ obtained after hydrothermal treatment (T = 150°C and t = 21 days) under air atmosphere in hydrochloric medium and with pH = 7.0 (10) (b).

Characterization of $CeSiO_4$ samples

To summarize, the multiparametric study developed to prepare pure $CeSiO_4$ allowed to determine optimal conditions, which correspond to the following guidelines:

Figure 9. PXRD diagram, calculated and difference profile after Rietveld refinement obtained for $CeSiO_4$ prepared under hydrothermal conditions (T = 150°C, t = 7 days) under air atmosphere in nitric medium and with pH = 7.0 starting from A-$Ce_2Si_2O_7$ precursor (10).

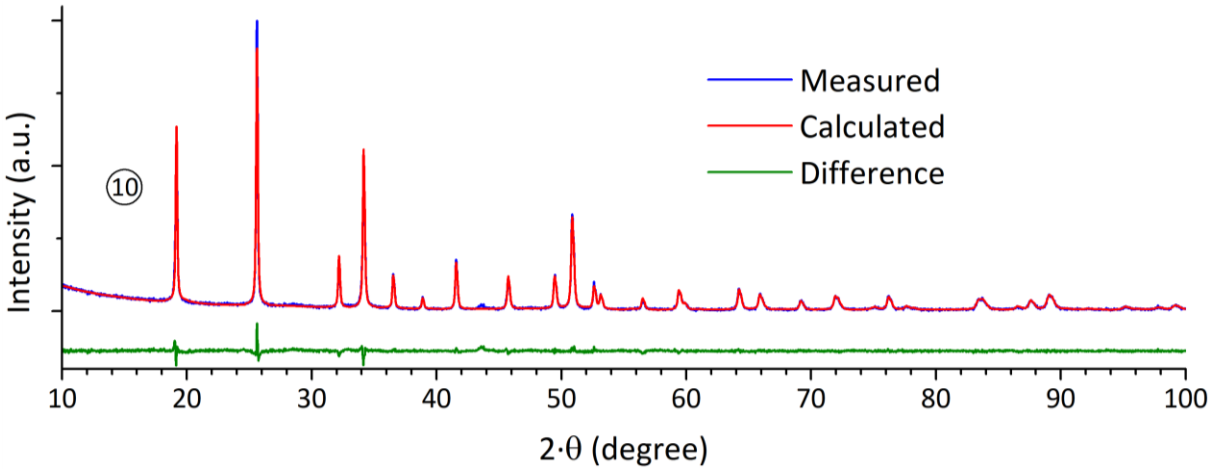

- A-$Ce_2Si_2O_7$ or $Ce_{4.67}(SiO_4)_3O$ used as Ce(III) starting precursors due to their favorable behavior (in terms of kinetics) during dissolution tests;
- nitric medium, to be preferred over hydrochloric one;
- hydrothermal treatment in air with a starting pH value adjusted to 7.0, a temperature of 150°C and maintained for at least 3 days.

For such optimized conditions, the Rietveld refinement of XRD data led to the following unit cell parameters: a = 6.9523(2) Å and c = 6.2036(2) Å, i.e. V = 300.06(2) $Å^3$ (**Figure 9**). These values is in good agreement with those obtained when using aqueous Ce(III) precursors [30] (a = 6.9603(1) Å and c = 6.1946(2) Å, i.e. V = 300.11(2) $Å^3$) and with those reported by Skakle et al. [9] (a = 6.9564(3) Å and c = 6.1953(4) Å, i.e. V = 299.80(3) $Å^3$). Moreover, infrared and Raman spectra recorded on these samples were characteristic of the features obtained for $CeSiO_4$ [30] (**Table S3**, **Figure S8** and **Figure S9**).

In order to complete the characterization of pure $CeSiO_4$, XANES and EXAFS experiments were performed at the Ce L_{III} edge. The sample studied was prepared after hydrothermal treatment in nitric medium (150°C, 7 hours, pH = 7) starting from A-$Ce_2Si_2O_7$. On the XANES spectra, the $CeSiO_4$ sample is characterized by a white line double peaks of roughly equal intensity with maxima at 5731 eV and 5738 eV (**Figure 10**). These double peaks are characteristic of tetravalent cerium corresponding to the $2p_{3/2} \rightarrow (4fL)5d$, and $2p_{3/2} \rightarrow (4f^0)5d$ electron transitions (L denotes relaxation transition of an electron from oxygen 2p to cerium 4f orbital) and their locations in good agreement with literature references, while trivalent cerium would be characterized by a single peak at 5727 eV (originating from the electron transition $2p_{3/2} \rightarrow (4f^1)5d$) (**Figure 10**).[38-40] Therefore, the XANES spectra tends to confirm the oxidation state +IV expected for $CeSiO_4$.

It could also be noticed that the shoulder usually observed at 5728 eV on the CeO_2 spectra (used as Ce(IV) reference in **Figure 10**), was not observed for $CeSiO_4$, probably because of the differences of Ce-O bonds local geometry in these two phases.

In order to confirm the Ce environment in $CeSiO_4$, pseudo-radial distribution function was determined from the Fourier transform of the EXAFS spectrum (k = 2–10 $Å^{-1}$). The data analysis was based on the model structure reported in the literature for the crystal structure of $CeSiO_4$.[9] Only Debye-Waller factors were adjusted variables whereas coordination numbers and distances were fixed to crystallographic values.

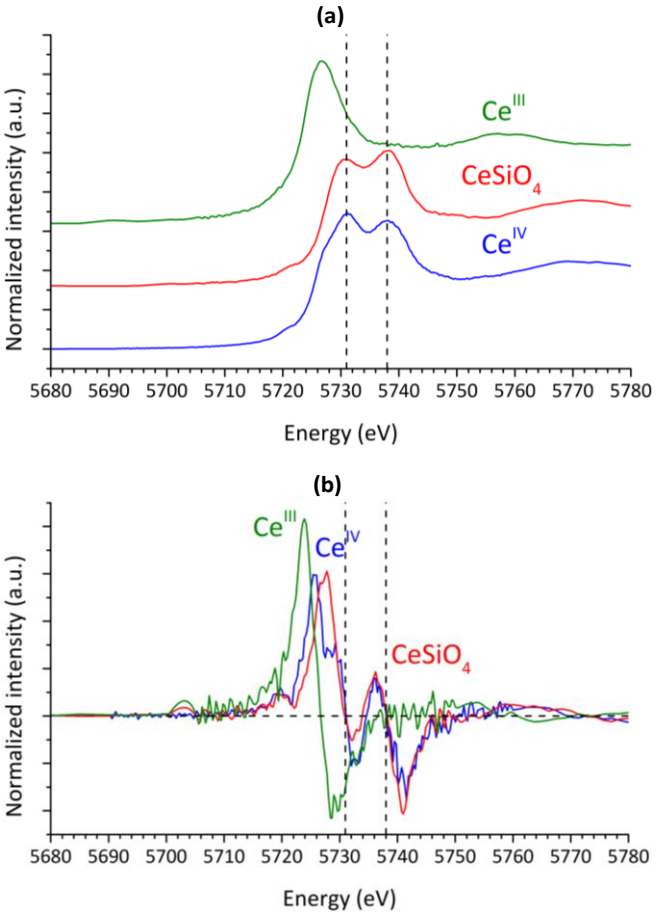

Figure 10. Ce L_{III} edge XANES spectrum (a) and respective first derivative (b) of Ce(III) and Ce(IV) references [40] and $CeSiO_4$ prepared under hydrothermal conditions (T = 150°C, t = 7 days) in nitric medium and with pH = 7.0, starting from A-$Ce_2Si_2O_7$ precursor (10).

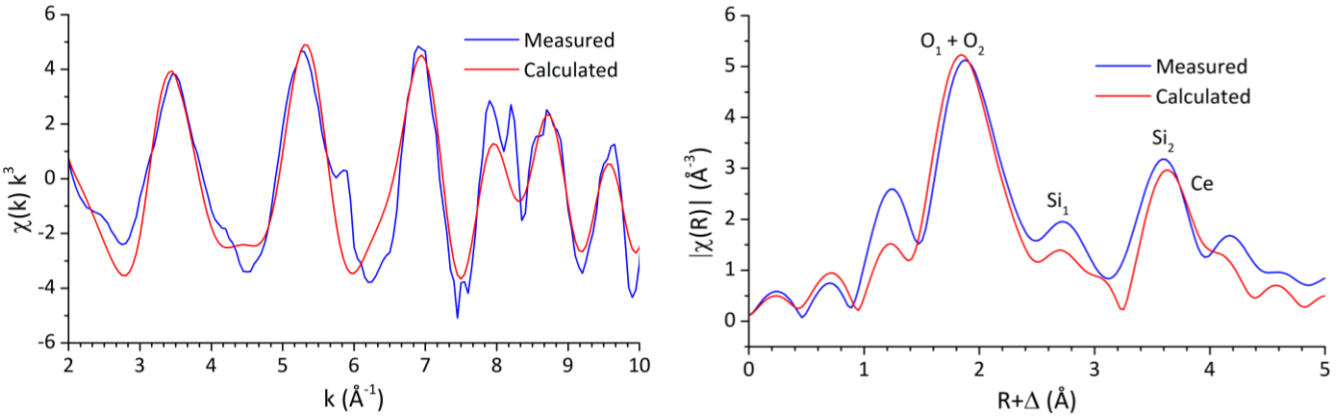

Figure 11. Cerium L_{III} EXAFS spectrum 2 Å < k < 10 $Å^{-1}$ (a) and corresponding Fourier transform (b) of $CeSiO_4$ prepared under hydrothermal conditions (T = 150°C, t = 7 days) under air atmosphere in nitric medium and with pH = 7.0, starting from A-$Ce_2Si_2O_7$ precursor (10).

Table 2. Structural parameters determined for $CeSiO_4$ sample. The values fixed for the simulations have been marked by an asterisk. $\Delta E_{k=0}$ = 4 eV ; F = 0.13 ; S_0^2 = 0.8.

	R (Å)	N	σ^2 (Å²)
Ce-O_1	2.2740 *	4 *	0.007 (5)
Ce-O_2	2.3645 *	4 *	0.006 (5)
Ce-Si_1	3.0976 *	2 *	0.001 (1)
Ce-Si_2	3.8075 *	4 *	0.003 (13)
Ce-Ce	3.8075 *	4 *	0.013 (13)

The spectra obtained from these simulations were found to be in good agreement with the experimental data (**Figure 11** and **Table 2**). The first peak was assigned to the oxygen atoms present in the first coordination sphere of cerium whereas the two following peaks were attributed to the silicon atoms present in the second coordination sphere, which correspond to bidentate and monodentate silicate bonds, respectively. At longer distance, a third contribution was associated to the Ce-Ce interactions. All of these results confirmed the formation of a zircon-type $CeSiO_4$ ($I4_1/amd$ space group), resulting from the oxidation of Ce(III) into Ce(IV) under hydrothermal conditions.

Discussion regarding the formation mechanism of $CeSiO_4$

According to the SEM observations, it may be inferred that the formation of $CeSiO_4$ relies on the low dissolution rates of the Ce(III) silicate starting precursor. This mechanism could correspond to the oxidative dissolution of Ce(III) silicate starting precursors, leading to the formation of Ce(IV)-silicate aqueous species which then precipitate as $CeSiO_4$. However, due to the suspected very low solubility of Ce(IV) silicate species,[30] the precipitation of $CeSiO_4$ in the near field of the precursor and then the formation of a passivating layer on its surface may be expected with this mechanism. However, since no passivating layer was observed, a chemical path through aqueous Ce(III) silicate intermediate species seems to be more likely.

The precursors dissolution could also correspond to the hydrolysis of the Si-O-Si bonds, which could exist for all Ce(III) silicate species, and then could lead to the release of Ce(III) silicate based complexes in the reactive media. These complexes are subsequently oxidized to form Ce(IV) silicate species which play a key role during the precipitation of $CeSiO_4$, as already described for thorium and uranium (IV) silicates.[41-43] The formation of Ce(IV) species may be enhanced by oxidizing species such as nitrogen based species coming from the decomposition of nitric acid and O_2 from air.
According to this hypothesis, the corresponding formation mechanism may be explained by the following reactions:

$$[\text{Ce(III)-silicate precursor}]_{solid} \leftrightharpoons [\text{Ce(III)-silicate complex}]_{aq}$$
$$[\text{Ce(III)-silicate complex}]_{aq} \leftrightharpoons [\text{Ce(IV)-silicate complex}]_{aq} + e^-$$
$$[\text{Ce(IV)-silicate complex}]_{aq} \leftrightharpoons [\text{Ce(IV)-silicate}]_{solid}$$

Since no aqueous characterization allowed us to identify the intermediate species, their nature remains unknown. Indeed, Ce(III) silicate complexes chemistry is poorly documented. However, based on the data reported for M(III) silicate aqueous chemistry,[44] the formation of $Ce^{III}(OSi(OH)_3)_n^{3-n}$ complex in solution could be suspected.[30] Moreover, the complexation by the nitrate anions must also be considered.
The aqueous Ce(III) species oxidation in nitric reactive media is most probably correlated to the reduction of nitrate ions through the following reactions [1]:

$HNO_3 + H^+ + e^- \leftrightharpoons ½\ N_2O_4 + H_2O$ E° = 0.803 V/ENH
$HNO_3 + 2\ H^+ + 2\ e^- \leftrightharpoons HNO_2 + H_2O$ E° = 0.934 V/ENH
$HNO_3 + 3\ H^+ + 3\ e^- \leftrightharpoons NO + 2\ H_2O$ E° = 0.957 V/ENH

The oxygen dissolved in the reactive media may also be involved in the oxidation of Ce(III).[1] It may, more precisely, explain the formation of $CeSiO_4$ in hydrochloric reactive media.

$½\ O_2 + 2\ H^+ + 2\ e^- \leftrightharpoons H_2O$ E° = 1.229 V/ENH

As mentioned for the speciation of Ce(IV), there is only little data in the literature concerning nitrate and hydroxo ions [45-49] and only extrapolated ones for silicate complexes.[30] However, it is known that for actinides and lanthanides, the complexation for M(IV) is much more important than for M(III).[44] This higher complexation obtained for M(IV)

compared to M(III) would, therefore, lead to an apparent decrease of the potential associated with the redox couple.[1, 50]

$Ce^{4+} + e^- \leftrightharpoons Ce^{3+}$ $E° = 1.72$ V/ENH

Indeed, as observed during the precipitation of CeO_2 at pH > 4 from Ce(III) reactants under aerated conditions,[46] the precipitation of $CeSiO_4$ may be explained by the complexation of Ce(IV) in solution and a very low solubility of Ce(IV)-silicate aqueous species. It is noteworthy to mention that the Ce(IV)/Ce(III) standard potential may also be modified under hydrothermal conditions.

As reported in our previous study, $CeSiO_4$ was stable during hydrothermal treatment at 250°C.[30] Therefore, the temperature limit observed for the conversion of Ce(III) silicate into $CeSiO_4$ was probably due to the destabilization of aqueous Ce(III) (and/or Ce(IV)) silicate intermediates for T > 150°C, and also of aqueous Ce(IV) silicate species with respect to hydroxide ones. In this context, the small amounts of $CeSiO_4$ observed for T > 150°C were surely formed during the beginning of the hydrothermal treatment (i.e. during the rise of temperature).

From a more general point of view, the formation of $CeSiO_4$ from Ce(III) silicate solid precursors appeared to be more efficient and easier than working directly from aqueous Ce(III) precursors. Indeed, this original way of preparation enabled to work on a wider pH range with a good recovery yield and without any constraint coming from the working atmosphere. This difference may result from the slow dissolution and oxidation (or oxidative dissolution) of Ce(III) starting precursors, leading to low concentrations in the reactive media which disfavored the cerium (IV) and cerium (III) hydrolysis.

Conclusions

$CeSiO_4$ was successfully formed from several solid Ce(III) based precursors, i.e. Ce_2SiO_5, $Ce_{4.67}(SiO_4)_3O$, A-$Ce_2Si_2O_7$ and G-$Ce_2Si_2O_7$ after hydrothermal treatment under air atmosphere. For several of them, their slow conversion allowed the preparation of single phase $CeSiO_4$ with higher recovery yields compared to those obtained when starting from mixtures of cerium and silicate solutions. The optimized conditions to form pure $CeSiO_4$ were based on hydrothermal treatment for 7 days at T ≤ 150°C (nitric medium) starting from A-$Ce_2Si_2O_7$ or $Ce_{4.67}(SiO_4)_3O$ precursor. Since $CeSiO_4$ was not obtained from Ce(IV) precursors due to the formation of CeO_2, as a consequence of the rapid hydrolysis of Ce(IV), the redox state of cerium in the starting precursor appeared as a key parameter. The formation of $CeSiO_4$ was directly correlated to the formation of Ce(III) silicate aqueous species which were slowly oxidized *in situ* during the hydrothermal treatment to form Ce(IV) silicate.

In addition, the reactivity of such Ce(III)-based silicates in representative conditions of environmental situations (pH = 7 and 60°C ≤ T ≤ 150°C) raises important questions about their evolution in conditions characteristic for several of their reported applications (including wet environments) [15, 16, 18-25]. It can also pave the way to a better understanding of the potential reactivity of actinide(III) silicate phases such as the solid Pu(III) silicate phases obtained by Fortner et al. by vapor phase hydration of borosilicate glasses [51, 52] and, therefore, of the behavior of plutonium in nuclear waste repository conditions.

Conflicts of interest

There are no conflicts to declare.

Acknowledgements

The authors would like to thank R. Podor, J. Lautru and V. Trillaud (from ICSM) for supporting SEM experiments.

Notes and references

1. D. R. Lide, *CRC Handbook of Chemistry and Physics*, CRC press, Boca Raton (FL), USA, 2005.
2. L. R. Morss, N. M. Edelstein, J. Fuger and J. J. Katz, 2006.
3. I. B. de Alleluia, Ph.D. Thesis. Fakultät für Chemie der Universität Karlsruhe, 1979.
4. I. B. de Alleluia, U. Berndt and C. Keller, *Revue de Chimie Minérale*, 1983, **20**, 441-448.
5. T. Uchida, S. Nakamichi, T. Sunaoshi, K. Morimoto, M. Kato and Y. Kihara, *IOP Conference Series: Materials Science and Engineering*, 2010, **9**.
6. C. Keller, *Nukleonik*, 1963, **5**, 41-48.
7. R. J. Finch and J. M. Hanchar, *Reviews in Mineralogy and Geochemistry*, 2003, **53**, 1-25.
8. J. A. Speer, *Reviews in Mineralogy and Geochemistry*, 1980, **5**, 113-135.
9. J. M. S. Skakle, C. L. Dickson and F. P. Glasser, *Powder diffraction*, 2000, **15**, 234-238.
10. C. Hennig, S. Weiss, D. Banerjee, E. Brendler, V. Honkimäki, G. Cuello, A. Ikeda-Ohno, A. C. Scheinost and H. Zänker, *Geochimica et Cosmochimica Acta*, 2013, **103**, 197-212.
11. I. Dreissig, S. Weiss, C. Hennig, G. Bernhard and H. Zänker, *Geochimica et Cosmochimica Acta*, 2011, **75**, 352-367.
12. R. Husar, S. Weiss, C. Hennig, R. Hübner, A. Ikeda-ohno and H. Zänker, *Environmental Science & Technology*, 2015, **49**, 665-671.
13. H. Zänker and C. Hennig, *Journal of Contaminant Hydrology*, 2014, **157**, 87-105.
14. H. Zänker, S. Weiss, C. Hennig, V. Brendler and A. Ikeda-Ohno, *Chemistry Open*, 2016, **5**, 174-182.
15. J. Felsche, *Die Naturwissenschaften*, 1969, **56**, 325-326.
16. A. C. Tas and M. Akinc, *Powder diffraction*, 1992, **7**, 219-222.
17. H. A. M. van Hal and H. T. Hintzen, *Journal of Alloys and Compounds*, 1992, **179**, 77-85.
18. A. C. Tas and M. Akinc, *Journal of the American Ceramic Society*, 1994, **77**, 2968-2970.
19. A. C. Tas and M. Akinc, *Journal of the American Ceramic Society*, 1994, **77**, 2953-2960.
20. M. Ghannadi Marageh, S. Waqif Husain, A. R. Khanchi and S. J. Ahmady, *Applied Radiation and Isotopes*, 1996, **47**, 501-505.
21. L. Kępiński, D. Hreniak and W. Stręk, *Journal of Alloys and Compounds*, 2002, **341**, 203-207.

22. L. Kępiński, M. Wołcyrz and M. Marchewka, *Journal of Solid State Chemistry*, 2002, **168**, 110-118.
23. S. Zec and S. Boskovic, *Journal of Materials Science*, 2004, **39**, 5283-5286.
24. S. Zec, S. Bošković, Ž. Bogdanov and N. Popović, *Materials Chemistry and Physics*, 2006, **95**, 150-153.
25. S. Zec, S. Bošković, M. Hrovat and M. Kosec, *Journal of the European Ceramic Society*, 2007, **27**, 523-526.
26. C. Lopez, Ph.D. Thesis. Université de Paris XI, 2002.
27. Y. Ding, X. Lu, H. Tu, X. Shu, H. Dan, S. Zhang and T. Duan, *Journal of the European Ceramic Society*, 2015, **35**, 2153-2161.
28. J. Schlüter, T. Malcherek and T. A. Husdal, *Neues Jahrbuch für Mineralogie - Abhandlungen*, 2009, **186**, 195-200.
29. C. L. Dickson and F. P. Glasser, *Cement and Concrete Research*, 2000, **30**, 1619-1623.
30. P. Estevenon, E. Welcomme, S. Szenknect, A. Mesbah, P. Moisy, C. Poinssot and N. Dacheux, *Dalton Transactions*, 2019, **48**, 7551-7559.
31. C. Frontera and J. Rodriguez-Carvajal, *Physica B: Condensed Matter*, 2003, **335**, 219-222.
32. C. Artini, M. Pani, M. M. Carnasciali, M. T. Buscaglia, J. R. Plaisier and G. A. Costa, *Inorganic Chemistry*, 2015, **15**, 4126–4137.
33. B. Ravel and M. Newville, *Journal of Synchrotron Radiation*, 2005, **12**, 537–541.
34. A. L. Ankudinov, B. Ravel, J. J. Rehr and S. D. Conradson, *Physica B: Condensed Matter*, 1998, **58**, 7565−7576.
35. E. D. A. Ferriss, R. C. Ewing and U. Becker, *American Mineralogist*, 2010, **95**, 229-241.
36. S. Cotton, *Lanthanide and actinide chemistry*, 2006.
37. J. P. Pupin, *Contributions to Mineralogy and Petrology*, 1980, **73**, 207-220.
38. Y. Takahashi, H. Shimizu, A. Usui, H. Kagi and M. Nomura, *Geochimica et Cosmochimica Acta*, 2000, **64**, 2919-2935.
39. X. Guo, A. H. Tavakoli, S. Sutton, R. K. Kukkadapu, L. Qi, A. Lanzirotti, M. Newville, M. Asta and A. Navrotsky, *Chemistry of Materials*, 2014, **26**, 1133-1143.
40. T. V. Plakhova, A. Y. Romanchuk, S. N. Yakunin, T. Dumas, S. Demir, S. Wang, S. G. Minasian, D. K. Shuh, T. Tyliszczak, A. A. Shiryaev, A. V. Egorov, V. K. Ivanov and S. N. Kalmykov, *Journal of Physical Chemistry C*, 2016, **120**, 22615-22626.
41. P. Estevenon, E. Welcomme, S. Szenknect, A. Mesbah, P. Moisy, C. Poinssot and N. Dacheux, *Inorganic Chemistry*, 2018, **57**, 9393-9402.
42. P. Estevenon, E. Welcomme, S. Szenknect, A. Mesbah, P. Moisy, C. Poinssot and N. Dacheux, *Inorganic Chemistry*, 2018, **57**, 12398-12408.
43. A. Mesbah, S. Szenknect, N. Clavier, J. Lozano-Rodriguez, C. Poinssot, C. Den Auwer, R. C. Ewing and N. Dacheux, *Inorganic Chemistry*, 2015, **54**, 6687-6696.
44. P. Thakur, D. K. Singh and G. R. Choppin, *Inorganica Chimica Acta*, 2007, **360**, 3705-3711.
45. S. A. Hayes, P. Yu, T. J. O'Keefe, M. J. O'Keefe and J. O. Stoffer, *Journal of The Electrochemical Society*, 2006, **149**, C623-C630.
46. B. Bouchaud, J. Balmain, G. Bonnet and F. Pedraza, *Journal of Rare Earths*, 2012, **30**, 559-562.
47. S. Bayulken and A. S. Sarac, *Turkish Journal of Chemistry*, 1996, **20**, 111-117.
48. B. D. Blaustein and J. W. Gryder, *Journal of the American Ceramic Society*, 1957, **79**, 540-547.
49. L. O. Tuazon, Ph.D. Thesis. Iowa State College, 1959.
50. N. A. Piro, J. R. Robinson, P. J. Walsh and E. J. Schelter, *Coordination Chemistry Reviews*, 2014, **260**, 21-36.
51. J. A. Fortner, C. J. Mertz, A. J. Baker, R. J. Finch and D. B. Chamberlain, *Materials Research Society, Symposium Proceedings*, 1999, **608**, 739-744.
52. J. A. Fortner, C. J. Mertz, D. C. Chamberlain and J. K. Bates, *Plutonium Futures - The Science, Santa Fe*, 1997.